Mössbauer and EPR Study of the Ni-Activated α-Subunit of Carbon Monoxide Dehydrogenase from *Clostridium thermoaceticum*

Jinqiang Xia,[†] Zhengguo Hu,[‡] Codrina V. Popescu,[‡] Paul A. Lindahl,[†] and Eckard Münck*[,‡]

Contribution from the Departments of Chemistry, Texas A & M University, College Station, Texas 77843, and Carnegie Mellon University, Pittsburgh, Pennsylvania 15213

Received March 31, 1997. Revised Manuscript Received June 23, 1997[⊗]

Abstract: The A-center of carbon monoxide dehydrogenase (CODH) resides in the enzyme's α-subunit and is responsible for the acetyl-CoA synthase activity. The center comprises a Ni site and an iron−sulfur cluster. We have isolated the α-subunit using both continuous and discontinuous electrophoresis methods. When incubated with CO, samples prepared using continuous gels attain the A_{red}-CO state that exhibits an $S = {}^1/_2$ EPR feature ($g =$ 2.048, 2.046, 2.021) similar to the so-called NiFeC signal of native CODH. Both signals consistently quantify to <0.4 spin/α. In order to elucidate the structure of the A-cluster and to understand the cause of the substoichiometric spin intensities, we have studied the α-subunit with Mössbauer and EPR spectroscopy. As found for CODH, populations of isolated α are heterogeneous: they contain two major A-cluster forms designated nonlabile and Ni-labile. In native CODH, only the Ni-labile form develops the NiFeC signal and exhibits catalytic activity. Oxidized samples of α exhibit Mössbauer spectra ($S = 0$, $\Delta E_Q = 1.08$ mm/s, $\delta = 0.45$ mm/s) typical of $[Fe_4S_4]^{2+}$ clusters. Upon reduction with dithionite, the Fe_4S_4 cluster of nonlabile A-clusters exhibits Mössbauer (average $\Delta E_Q = 1.0$ mm/s, $\delta = 0.54$ mm/s) and EPR properties similar to those of $S = {}^3/_2$ $[Fe_4S_4]^+$ cubanes; in contrast, Ni-labile clusters are not reducible by dithionite. Treatment with CO yielded a sample for which 40% of the Fe was associated with A_{red}-CO, while 47% of the clusters (the nonlabile form) remained oxidized. Thus, the presence of nonlabile A-clusters is largely responsible for the low spin intensities of the NiFeC signal. Upon formation of A_{red}-CO, the Fe_4S_4 portion of the A-cluster exhibits ^{57}Fe magnetic hyperfine interactions; the cluster sites divide into equivalent pairs with (isotropic) $A_A = A_B = -34.2$ MHz and $A_C = A_D = +26.8$ MHz. However, the values of ΔE_Q and δ show that the cluster has remained in the $[Fe_4S_4]^{2+}$ state. We explain these observations with an electronic model that considers a $Ni^+-X-[Fe_4S_4]^{2+}$ assembly for which the Ni^+ is exchange-coupled with one Fe site of the cube through a bridging ligand (X). The coupling was found to be substantial, namely $|j| \approx 100$ cm^{-1} ($H_{NiFe} = j\mathbf{S}_{Ni}\cdot\mathbf{S}_{Fe}$). The Mössbauer spectra provide no evidence that CO is bound to the Fe_4S_4 cluster in the state A_{red}-CO, as has been concluded from resonance Raman studies [Qiu, D.; Kumar, M.; Ragsdale, S. W.; Spiro, T. G. *Science* 1994, *264*, 817−819]. We could not determine if the two metal centers are linked in the *oxidized* state (for either the Ni-labile or nonlabile form), but if they are, the Ni^{2+} must be low-spin ($S_{Ni} = 0$).

Introduction

Acetogenic bacteria such as *Clostridium thermoaceticum* can grow autotrophically, using the Wood/Ljungdahl pathway to synthesize acetyl-CoA from CO_2 and H_2. The central enzyme in this pathway, carbon monoxide dehydrogenase (CODH), catalyzes the reversible oxidation of CO to CO_2 and the synthesis of acetyl-CoA from CO, coenzyme A, and a methyl group donated from a corrinoid/iron−sulfur enzyme.[1]

Because CODH contains novel metal clusters and is one of only five naturally occurring Ni-containing enzymes, it has recently received considerable attention. CODH is a 310 000 Da $\alpha_2\beta_2$ tetramer containing ∼4 Ni, ∼24 Fe, and ∼24 S^{2-}, which are organized into three clusters named A, B, and C. The C-cluster is the active site for reversible CO_2 reduction/CO oxidation and is located in the β-subunit.[2−4] The B-cluster, also located in the β-subunit, is an $[Fe_4S_4]^{2+/+}$ cluster that functions in electron transfer.

The A-cluster is the active site for acetyl-CoA synthesis[5−7] and is located in the α-subunit.[4] It is stable in two redox states, namely an oxidized state (A_{ox}) and a one-electron reduced $S = {}^1/_2$ state (A_{red}-CO) that exhibits an EPR signal ($g = 2.08$, 2.07, and 2.03) known as the NiFeC signal.[8] A_{ox} can be transformed into A_{red}-CO by exposing the enzyme to CO.[6a,9] The electron required to reduce A_{ox} when CODH is exposed to CO is obtained by the oxidation of CO at the C-cluster.[10]

* To whom correspondence should be addressed. Phone: 412-268-5058. Fax: 412-268-1061. E-mail: em40@andrew.cmu.edu.
† Texas A & M University.
‡ Carnegie Mellon University.
⊗ Abstract published in *Advance ACS Abstracts,* August 15, 1997.

(1) Ragdale, S. W.; Kumar, M. *Chem. Rev.* **1996**, *96*, 2515−2539.
(2) Anderson, M. E.; De Rose, V. J.; Hoffman, B. M.; Lindahl, P. A. *J. Am. Chem. Soc.* **1993**, *115*, 12204−12205.
(3) Kumar, M.; Lu, W.-P.; Liu, L.; Ragsdale, S. W. *J. Am. Chem.* **1993**, *115*, 11646−11647.
(4) Xia, J.; Sinclair, J. F.; Baldwin, T. O.; Lindahl, P. A. *Biochemistry* **1996**, *35*, 1965−1971.
(5) Gorst, C. M.; Ragsdale, S. W. *J. Biol. Chem.* **1991**, *266*, 20687−20693.
(6) (a) Shin, W.; Lindahl, P. A. *Biochemistry* **1992**, *31*, 12870−12875. (b) Shin, W.; Stafford, P. R.; Lindahl, P. A. *Biochemistry* **1992**, *31*, 6003−6011.
(7) Shin, W.; Anderson, M.; Lindahl, P. A. *J. Am. Chem. Soc.* **1993**, *115*, 5522−5526.
(8) (a) Lindahl, P. A.; Münck, E.; Ragsdale, S. W. *J. Biol. Chem.* **1990**, *265*, 3873−3879. (b) Lindahl, P. A.; Ragsdale, S. W.; Münck, E. *J. Biol. Chem.* **1990**, *265*, 3880−3888. (c) Ragsdale, S. W.; Wood, H. G.; Antholine, W. E. *Proc. Natl. Acad. Sci. U.S.A.* **1985**, *82*, 6811−6814.
(9) (a) Ragsdale, S. W.; Ljungdahl, L. J.; der Vartanian, D. V. *Biochem. Biophys. Res. Commun.* **1982**, *108*, 658−663. (b) Ragsdale, S. W.; Ljungdahl, L. J.; der Vartanian, D. V. *Biochem. Biophys. Res. Commun.* **1983**, *115*, 658−665. (c) Ragsdale, S. W.; Wood, H. G. *J. Biol. Chem.* **1985**, *260*, 3970−3977.

S0002-7863(97)01025-1 CCC: $14.00

Ragsdale *et al.*[9] discovered that the NiFeC signal exhibits magnetic hyperfine broadening when the A-cluster is enriched in ^{61}Ni ($I = {}^3/_2$) or ^{57}Fe ($I = {}^1/_2$) or when CODH is reduced with ^{13}CO ($I = {}^1/_2$). This indicates that A_{red}-CO contains Ni and Fe in an exchange-coupled assembly to which CO is bound. Lindahl *et al.*[8b] studied CODH with Mössbauer spectroscopy and found that the irons of A_{red}-CO have isomer shifts and quadrupole splittings typical of those observed for $[Fe_4S_4]^{2+}$ clusters. However, while magnetically isolated $[Fe_4S_4]^{2+}$ clusters are diamagnetic, the iron sites of A_{red}-CO exhibit substantial magnetic hyperfine interactions. The magnetic hyperfine coupling constants determined from Mössbauer spectroscopy were subsequently confirmed by an ENDOR study of the enzyme; this study also demonstrated that the A-cluster contains at least three Fe sites.[11]

For reasons that are not well understood, the spin concentration of the NiFeC signal is much lower than expected; double integrations yield <0.3 spin/$\alpha\beta$ (average about 0.2 spin/$\alpha\beta$) rather than the expected value of 1 spin/$\alpha\beta$.[8] The ability of the A-cluster to exhibit the NiFeC signal is readily destroyed by oxygen, and Shin and Lindahl thought that oxygen damage was responsible for the substoichiometric spin concentration.[12] However, the intensity remained low ($\sim$0.2 spin/$\alpha\beta$) throughout an enzyme purification for which it was known that the enzyme had not been inactivated by oxygen.[12] Thus, the substoichiometric spin concentration seems to arise from factors operating prior to purification.

Our previous Mössbauer study suggested that enzyme populations are heterogeneous and that this heterogeneity is at the root of the low spin intensity. Lindahl *et al.*[8] found that the fraction of Mössbauer absorption that could unambiguously be associated with A_{red}-CO corresponded to $\sim$18% of the Fe in the sample and that a fraction of the A-cluster in the sample was not reducible by CO. The spin concentration of the NiFeC signal of the same sample corresponded to only 0.35 spin/$\alpha\beta$, and thus the possibility arose that only a fraction ($\sim$35%) of enzyme molecules were capable of attaining the state that yielded the NiFeC signal. Further support for this came when 1,10-phenanthroline (phen) was found to selectively remove the Ni of the A-cluster.[6,7] Phen-treated enzyme lacks CO/acetyl-CoA exchange activity and the NiFeC signal but has full CO oxidation activity. Moreover, Ni ions insert into the empty labile site of the A-cluster when phen-treated enzyme is incubated with aqueous Ni^{2+}. With Ni reinserted, CODH again catalyzes CO/acetyl-CoA exchange and exhibits the NiFeC signal. Surprisingly, only about 0.3 Ni/$\alpha\beta$ can be removed/reinserted. To explain the low NiFeC signal intensity and the heterogeneity indicated by the Mössbauer data, Shin and Lindahl suggested that only $\sim$30% of $\alpha\beta$ dimers had A-clusters containing a labile Ni and that the remainder contained structures grossly similar to the A-cluster but with nonlabile Ni ions.[7] These authors suggested that the Ni-labile A-clusters, if undamaged by oxygen, were catalytically active and able to exhibit the NiFeC signal, while nonlabile A-clusters and A-clusters damaged by oxygen were inactive and unable to exhibit the EPR signal.

Another puzzling aspect of the A-cluster is that the Mössbauer isomer shifts in both the A_{ox} and A_{red}-CO states are typical of Fe_4S_4 clusters in the 2+ core oxidation state. Münck and coworkers[8] suggested that the electron used to reduce A_{ox} localizes on the Ni site of the A-cluster rather than on the Fe_4S_4 moiety, generating a Ni^+ exchange-coupled to an $[Fe_4S_4]^{2+}$ cluster in a bridged $Ni^+-X-[Fe_4S_4]^{2+}$ assembly. This proposal was consistent with the XAS spectra of Bastian *et al.*[14] (which lacked evidence for a short 2.7 Å Ni−Fe interaction and possibly included a long 3.2 Å Ni−Fe interaction) and with their suggestion that the Ni ion in the A-cluster was in some manner bridged to (rather than incorporated into) the Fe−S moiety. The proposed spin-coupling mechanism was similar to that developed to explain the spectroscopic data obtained for *Escherichia coli* sulfite reductase;[15] this theory postulated a covalent link between the siroheme and an $[Fe_4S_4]^{2+}$ cluster, a conjecture confirmed by subsequent X-ray diffraction studies of the enzyme.[35] However, given the substantial spectral interference due to the other clusters in CODH as well as the difficulties caused by heterogeneity, Lindahl *et al.* cautioned that much stronger evidence for a coupled $Ni-[Fe_4S_4]^{2+}$ chromophore was required.[8]

Recently, Xia *et al.*[4] reported that small amounts of the detergent SDS decompose CODH ($\alpha_2\beta_2$) into α and $\alpha\beta_2$. The isolated α-subunit was reported to contain about one Ni and four Fe.[16] The Ni appears to be redox-inactive in the 2+ state, with two S ligands at 2.19 Å and two N/O ligands at 1.90 Å in a distorted tetrahedral geometry. UV−vis, EPR, and EXAFS spectra all suggest that the irons in α are organized into an $[Fe_4S_4]^{2+/+}$ cluster that has an $S = {}^3/_2$ ground state in the dithionite-reduced form.[16]

Xia and Lindahl[17] found that incubating isolated α with aqueous Ni^{2+}, CO, and a catalytic amount of CODH yields an EPR signal ($g = 2.05, 2.02$) with properties very similar to those of the NiFeC signal. This so-called pseudo-NiFeC signal (pNiFeC) of "activated" α exhibits hyperfine broadening when ^{13}CO, aqueous ^{61}Ni, or ^{57}Fe-enriched α is used. These properties indicate that the A-cluster of isolated α has the same basic structure as the A-cluster of native enzyme, namely of a Ni ion spin-coupled to a single Fe_4S_4 cluster. The activated α-subunit had no catalytic activity, but the $\alpha\beta_2$ trimer, when similarly activated, yielded the NiFeC signal and had CO/acetyl-CoA exchange activity. This shows that a single A-cluster is sufficient for activity as long as β-subunits are attached to the α-subunit housing that cluster.

We have now investigated the properties of the isolated α-subunit using the combined Mössbauer/EPR approach. The present study was aimed at resolving the puzzle of the low spin concentration and the heterogeneity problem and elucidating further the structural features of the A-cluster and its redox properties. In this paper, we show that A_{red}-CO contains an Fe_4S_4 cluster in the 2+ state. We present a theory based on previous work on the exchange-coupled siroheme$-[Fe_4S_4]^{2+}$ chromophore that explains signs and magnitudes of the observed ^{57}Fe magnetic hyperfine coupling tensors. Our analysis shows that the exchange interactions between the Ni^+ site and Fe_D of the cluster are quite strong, $\sim$100 cm^{-1}$\mathbf{S}_{Ni}\cdot\mathbf{S}_D$. We also show that only a fraction of α-subunits contain Ni-labile A-clusters and that this is largely responsible for the observed low spin intensity.

(10) Anderson, M. E.; Lindahl, P. A. *Biochemistry* **1994**, *33*, 8702−8711.
(11) Fan, C.; Gorst, C. M.; Ragsdale, S. W.; Hoffman, B. M. *Biochemistry* **1991**, *30*, 431−435.
(12) Shin, W.; Lindahl, P. A. *Biochim. Biophys. Acta* **1993**, *1161*, 317−322.
(13) Hu, Z.; Spangler, N. J.; Anderson, M. E.; Xia, J.; Ludden, P.; Lindahl, P. A.; Münck, E. *J. Am. Chem. Soc.* **1996**, *118*, 830−845.
(14) Bastian, N. R.; Diekert, G.; Niederhoffer, E. C.; Teo, B. K.; Walsh, C. T.; Orme-Johnson, W. H. *J. Am. Chem. Soc.* **1988**, *110*, 5581−5582.
(15) Münck, E. In *Iron-Sulfur Proteins*; Spiro, T. G., Eds.; Wiley-Interscience: New York, 1982; Vol. 4, pp 148−175.
(16) Xia, J.; Dong, J.; Wang, S.; Scott, R. A.; Lindahl, P. A. *J. Am. Chem. Soc.* **1995**, *117*, 7065−7070.
(17) Xia, J.; Lindahl, P. A. *J. Am. Chem. Soc.* **1996**, *118*, 483−484.
(18) Lundie, L. L., Jr.; Drake, H. L. *J. Bacteriol.* **1984**, *159*, 700−703.
(19) Ramer, S. E.; Raybuck, S. A.; Orme-Johnson, W. H.; Walsh, C. T. *Biochemistry* **1989**, *28*, 4675−4680.
(20) Raybuck, S. A.; Bastian, N. R.; Orme-Johnson, W. H.; Walsh, C. T. *Biochemistry* **1988**, *27*, 2698−7702.

Experimental Procedures

Three batches of CODH were purified[12] (see also refs 18−20) from ^{57}Fe-enriched *C. thermoaceticum*. All were ∼90% pure according to SDS−PAGE. The ^{57}Fe-enriched batches 1−3 had CO oxidation activities of 220, 218, and 266 units/mg and CO/acetyl-CoA exchange activities of 0.07, 0.26, and 0.18 units/mg, respectively.[12] When reduced with CO, batches 2 and 3 exhibited NiFeC signals quantifying to 0.25 and 0.24 spin/αβ, respectively.

The α-subunits from batch 1 were isolated using discontinuous gel electrophoresis as described,[4] while those from batches 2 and 3 were isolated similarly but with the following modifications: A 9% polyacrylamide separating gel was prepared by mixing acrylamide/Bis premix (4.5 g of 37.1:1, BioRad) with 5 mL of 1 M boric acid, 5 mL of 0.5 M Tris (Trisma base, Sigma), 250 μL of 1 M DTT, and 20 μL of TEMED and diluting to 50 mL with water. After 5 min degassing, the solution was mixed with 12−14 μL of 1% ammonium persulfate and immediately poured into the gel tube. A solution (10 mL of 100 mM boric acid/50 mM Tris) was immediately and gently layered on top of the gel. Polymerization began after 5 min and was complete in ∼8 h. Upper electrode buffer was 100 mM boric acid, 50 mM Tris, and 5 mM DTT. Lower electrode buffer was identical except that it lacked DTT and contained 6 mM dithionite. The gel was prerun at 250 V for 2−2.5 h and cooled to 10−15 °C. CODH was incubated in 1000 equiv/αβ of SDS for 1 h, loaded on the gel, and electrophoresed at 180 V. The cell was disassembled after 3−4 h, and the fastest-migrating brown band, due to α, was isolated and electroeluted[4] using 5 mM DTT in the buffer. The α samples isolated from batches 2 and 3 were 70% and 80% pure according to SDS−PAGE and contained 3.9 Fe and 4.0 Fe, respectively, after correcting for the impurities and assuming that the impurities were devoid of metal ions. Metal and protein concentrations were determined as described.[16] EPR spin quantitations were performed as described previously[6a] and supported by spectral simulations with a program written by Dr. M. P. Hendrich. Mössbauer spectra were analyzed with the program WMOSS (WEB Research Co.)

The α-subunit isolated from batch 1, in 50 mM Tris pH 8, was oxidized with just enough thionin to cause the solution to turn slightly blue and then transferred into a Mössbauer cup and frozen. After analysis, the sample was thawed, reduced with dithionite (5 mM final), and refrozen. The α-subunits isolated from batch 2 were concentrated using a Centricon-100 (Amicon, Inc.), freed of dithionite by chromatography through Sephadex G25 (Pharmacia), equilibrated in 50 mM Tris-Cl, pH 8, and then reconcentrated. An aliquot (400 μL) of dithionite-free α was placed into a Mössbauer cup located in a 10 mL vial (Wheaton) and then mixed with Triton X-100 (50 μL of 200 mg/mL), $NiCl_2$ (50 μL of 10 mM), and native CODH (5 μL of 10 mg/mL). The Triton was added to minimize aggregation. The vial was sealed with a rubber septum and filled with 1 atm CO. After 4 h, 100 μL of the solution was injected into a capillary EPR tube (75 mm × 2 mm o.d.) filled with CO. The tube and cup were frozen within ∼2 min of each other in liquid N_2.

The dithionite-free α isolated from batch 3 (0.9 mL) was incubated for 4 h with Triton X-100 (0.1 mL of 200 mg/mL) and $NiCl_2$ (0.1 mL of 10 mM). An aliquot (200 μL) was oxidized by thionin (2.5 μL of 20 mM) and frozen in a Mössbauer cup. Another aliquot (550 μL) was mixed with 5 μL of 5 mg/mL CODH and injected into a Mössbauer cup located in a septum-sealed 10 mL vial filled with 1 atm CO. After 1 h, a portion (100 μL of 0.46 mM α) was transferred into a capillary EPR tube filled with CO. The cup and tube were frozen in liquid N_2 as above. After analysis, the sample of CO-treated α from batch 3 was thawed and refrozen five times in order to damage the Ni-labile A-clusters. Due to the ineffectiveness of this procedure, the sample was diluted into 100 mL of Tris pH 8 and incubated overnight at room temperature. The sample was concentrated using a Centricon, mixed with 5 μL of 10 mg/mL CODH, and then reexposed to CO as above. A portion was transferred to a capillary EPR tube, and both were frozen as above. The sample was devoid of the pNiFeC EPR signal.

Results

EPR and Mössbauer Studies of Oxidized and Reduced α-Subunit. We have prepared a batch of ^{57}Fe-enriched α-subunit for a combined EPR and Mössbauer study, using the discontinuous gel method described previously.[4] The zero-field Mössbauer spectrum, recorded at 4.2 K and shown in Figure 1, consists of a sharp quadrupole doublet with $\Delta E_Q = 1.08$ mm/s and $\delta = 0.45$ mm/s. The same ΔE_Q was obtained at 150 K. These parameters and the diamagnetic environment in which these irons reside (see below) are typical of $[Fe_4S_4]^{2+}$ clusters. Together with the metal content of the subunit (∼4 Fe/α) and other evidence mentioned in the Introduction, these results indicate that the α-subunit contains a single $[Fe_4S_4]^{2+}$ cluster. This conclusion is supported by EPR and Mössbauer studies of dithionite-reduced α-subunit.

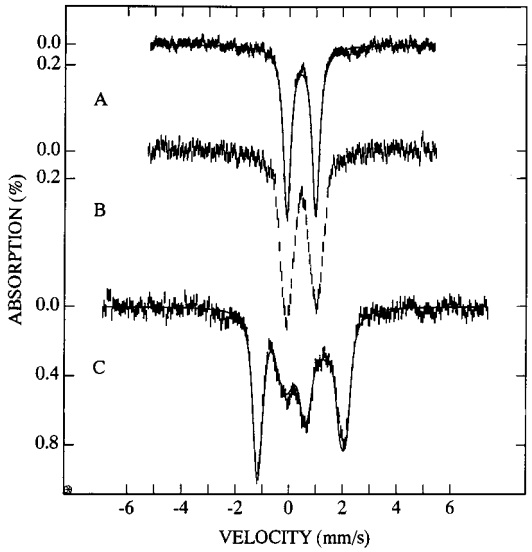

Figure 1. 4.2 K Mössbauer spectra of ^{57}Fe-enriched α-subunit recorded in 0.05 T (A,B) and 8.0 T (C) applied magnetic fields. The sample for A was prepared by *discontinuous* gel electrophoresis (batch 1), whereas that for B and C was prepared with *continuous* gel electrophoresis and activated with Ni^{2+} (batch 3). The solid line in spectrum A is a fit with $\Delta E_Q = 1.08$ mm/s and $\delta = 0.45$ mm/s. The doublet in Spectrum B has average $\Delta E_Q \approx 1.08$ mm/s and $\delta = 0.45$ mm/s. The solid line in spectrum C is a spectral simulation generated for $S = 0$ and $\Delta E_Q = 1.08$ mm/s, $\eta = 0.5$, $\delta = 0.45$ mm/s.

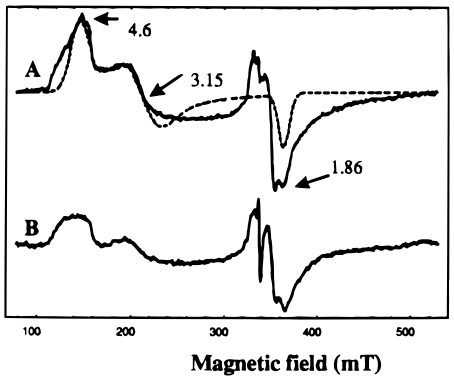

Figure 2. EPR spectra of dithionite-reduced α-subunit recorded at 10 K. Samples were prepared with discontinuous gel electrophoresis. (A) Spectrum of α-subunit containing Fe in natural abundance. The dashed line is a theoretical spectrum for an $S_{eff} = {}^1/_2$ species with $\mathbf{g} = (4.6, 3.20, 1.86)$ drawn to outline the main features of the $S = {}^3/_2$ component. (B) Spectrum of ^{57}Fe-enriched sample used for recording the Mössbauer spectra of Figure 3. Conditions: microwave power, 10 mW; frequency, 9.43 GHz.

Figure 2 shows 10 K EPR spectra of the dithionite-reduced α-subunit. The spectrum of Figure 2A was obtained for a sample containing ^{57}Fe in natural abundance, while that of Figure 2B was recorded for the ^{57}Fe-enriched sample of Figure

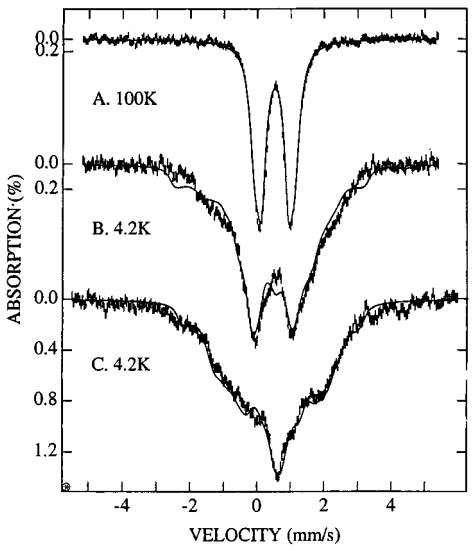

Figure 3. Mössbauer spectra of dithionite-reduced α-subunit (batch 1), prepared by the discontinuous gel method, recorded at the indicated temperatures in zero field (A) and in parallel fields of 0.05 T (B) and 8.0 T (C). The solid lines are spectral simulations using an $S = {}^3/_2$ spin Hamiltonian for $D = 4$ cm^{-1}, $E/D = 0.04$, and the following sets of hyperfine parameters for ΔE_Q, η, [A_x, A_y, A_z in MHz]. Site 1: 1.18 mm/s, −2.4, [−1.5, −0.65, −7.6]. Site 2: 1.18 mm/s, 0.4, [−17.4, −1, 0]. Site 3: 0.8 mm/s, −0.5, [−2.8, −7.8, −20]. Site 4: 0.8 mm/s, −0.2, [−10.7, −23, 0]. All isomer shifts were $\delta = 0.53$ mm/s, and line widths were 0.35 mm/s fwhm. *A*-values and zero-field splitting parameters are not unique; many different "reasonable" fits, involving four distinct iron sites, are possible.

3. The EPR spectra exhibit broad resonances centered around $g_{eff} = 4.6$ and 3.15. Such (effective) *g*-values can be attributed to the $M_S = \pm{}^1/_2$ doublet from an $S = {}^3/_2$ system for which $|D| \gg \beta$H and $E/D \approx 0.04$; signal shapes and *g*-values are similar to those observed for $[Fe_4S_4]^+$ cubanes with $S = {}^3/_2$.[13,21,22] The details of the spectra vary somewhat with the preparation, as is also apparent from comparison of the spectra in Figure 2 (the broader features of the spectrum in Figure 2B cannot be attributed to ^{57}Fe hyperfine interactions). The spectra of the $S = {}^3/_2$ species are not readily simulated by assuming contributions of two Kramers doublets from an $S = {}^3/_2$ system. To aid the reader with identifying the main features, we have added a spectral simulation (dashed line) for one doublet with effective *g*-values at 4.6, 3.2, and 1.86. The simulation outlines the essential features of the spectrum and highlights the presence of a shoulder at low field. This shoulder is too intense to be attributed to the $M_S = \pm{}^3/_2$ doublet,[23] but it is generally similar to the features exhibited by the majority $S = {}^3/_2$ species. The spectrum of Figure 2A also contains a contribution from an $S = {}^1/_2$ species with resonances around $g = 2.03$ and 1.94; simulations suggest that this species represents less than 3% of the total cluster population. We have observed the mentioned features, with slight variations, in all preparations examined, including the ^{57}Fe-enriched sample of Figure 2B.

The Mössbauer spectra of the dithionite-reduced α-subunit, shown in Figure 3, are also typical of $[Fe_4S_4]^+$ cubanes with $S = {}^3/_2$ ground states.[21,22] The 100 K spectrum consists of a quadrupole doublet which is best fit by assuming two components with $\delta(1) = 0.53$ mm/s, $\Delta E_Q(1) = 0.80$ mm/s and $\delta(2) = 0.53$ mm/s, $\Delta E_Q(2) = 1.18$ mm/s. These parameters are nearly identical to those of the $S = {}^3/_2$ $[Fe_4S_4]^+$ cluster of the Fe protein of nitrogenase, for which $\delta_1 = \delta_2 = 0.54$ mm/s, $\Delta E_Q(1) = 0.8$ mm/s, and $\Delta E_Q(2) = 1.2$ mm/s have been reported.[21] The 4.2 K spectra (Figure 3B,C) are rather featureless and not well resolved for any applied field up to and including 8.0 T. Because the spectra are poorly resolved and the magnitude of the zero field splitting parameter *D* is unknown, the spectral simulations by themselves are not likely to yield a unique parameter set. Nevertheless, the simulations presented in Figure 3 roughly represent the shape of the spectra and reveal two properties of the cluster. First, our simulations show that no excessive line widths or distributed parameters are required to fit the data. Second, all iron sites appear to have A-tensors with negative components, in accord with the data reported for other $S = {}^3/_2$ cubanes.[21,22]

Activation and Heterogeneity of α. Shin *et al.*[7] have reported that populations of native CODH contain two different forms of the A-cluster, called nonlabile and Ni-labile, and our studies of the isolated α-subunit can be similarly interpreted. The Ni-labile form of the α-subunit can react with CO in the presence of catalytic amounts of CODH (designated CO/CODH) to form the state A_{red}-CO that exhibits the pNiFeC signal. Removal of Ni from Ni-labile A-centers yields a form (Ni-depleted A-centers) that contains only the Fe_4S_4 cluster. The nonlabile form does not exhibit the pNiFeC signal and contains a Ni ion that cannot be removed with phenanthroline. Finally, exposure to oxygen or dilution of the protein converts the Ni-labile form into damaged A-centers, a form that is incapable of developing the NiFeC signal upon exposure to CO/CODH. (We have not studied the effects of dilution systematically but have noticed that preparations of α seem to exhibit higher pNiFeC signal intensities if they had not been diluted extensively or maintained in a diluted state for an extensive period during purification.)

Samples of α prepared with *discontinuous* gel electrophoresis (similar to those of Figures 1A, 2, and 3) afforded only weak (∼0.04 spin/α) pNiFeC signals when exposed to CO/CODH. These low values suggested that only ∼4% of α-subunits contained Ni-labile A-clusters and that the remainder contained either nonlabile, damaged, and/or Ni-depleted A-clusters. Even after activation with Ni^{2+}, the signal concentration increased to only 0.1 spin/α, suggesting that the majority of A-clusters in these samples were either nonlabile or damaged.

To achieve spin concentrations large enough to warrant a combined Mössbauer/EPR study of A_{red}-CO, an isolation procedure was developed that involves subjecting SDS-incubated enzyme to anaerobic, native, prerun, continuous polyacrylamide gel electrophoresis and then electroeluting α from the gel.[24] After activation with Ni^{2+}, α-subunit samples prepared in this manner exhibited pNiFeC signals with spin concentrations up to ∼0.3 spin/α. The EPR and Mössbauer studies reported below were carried out with samples prepared by *continuous* gel electrophoresis.

(21) Lindahl, P. A.; Day, E. P.; Kent, T. A.; Orme-Johnson, W. H.; Münck, E. *J. Biol. Chem.* **1985**, *260*, 11160−11173.

(22) Carney, M. J.; Papaefthymiou, G. C.; Spartalian, K.; Frankel, R. B.; Holm, R. H. *J. Am. Chem. Soc.* **1988**, *110*, 6084−6095.

(23) Rawlings, J.; Shah, V. K.; Chisnell, J. R.; Brill, W. J.; Zimmermann, R.; Münck, E.; Orme-Johnson, W. H. *J. Biol. Chem.* **1978**, *253*, 1001−1004.

(24) Two aspects of the earlier method seem to have damaged the Ni-labile A-clusters. First, discontinuous gels contain ammonium persulfate and TEMED, and these polymerization reagents may damage the A-cluster. Continuous gels, which are devoid of a stacking gel, can be freed of these reagents by passing current through them prior to applying the sample (called prerunning). Unfortunately, continuous gels have poorer resolving power than discontinuous ones, causing lower yields of α and greater contamination with the β-subunit. Second, in the earlier isolation method, samples were eluted from the gel in a very dilute state, and dilution has been found to damage Ni-labile A-clusters. The electroelution method concentrates the sample but strips the labile Ni from the A-cluster. The resulting Ni-depleted A-clusters are not damaged, in that they can be activated to the Ni-labile form by incubation with Ni^{2+}.

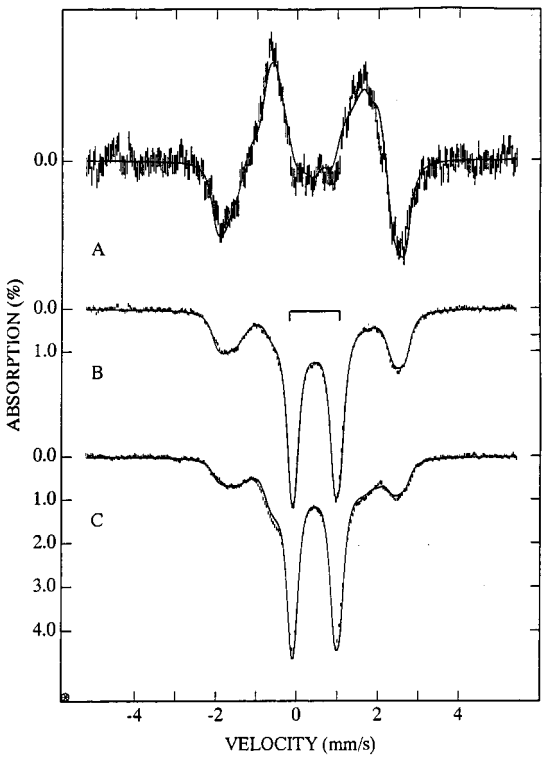

Figure 4. Mössbauer spectra of Ni^{2+}-activated α-subunit (batch 2) treated with CO/CODH. Spectra were recorded at 90 K in 0.05 T magnetic fields applied parallel (B) and perpendicular (C) to the incident γ-radiation. The spectrum shown in A was obtained by subtracting spectrum C from spectrum B; in this procedure, the contributions of the diamagnetic $[Fe_4S_4]^{2+}$ cluster (indicated by the bracket) and the Fe^{2+} contaminant cancel. The solid lines in Figures 4−6 are spectral simulations based on eq 1 using the parameters listed in Table 1.

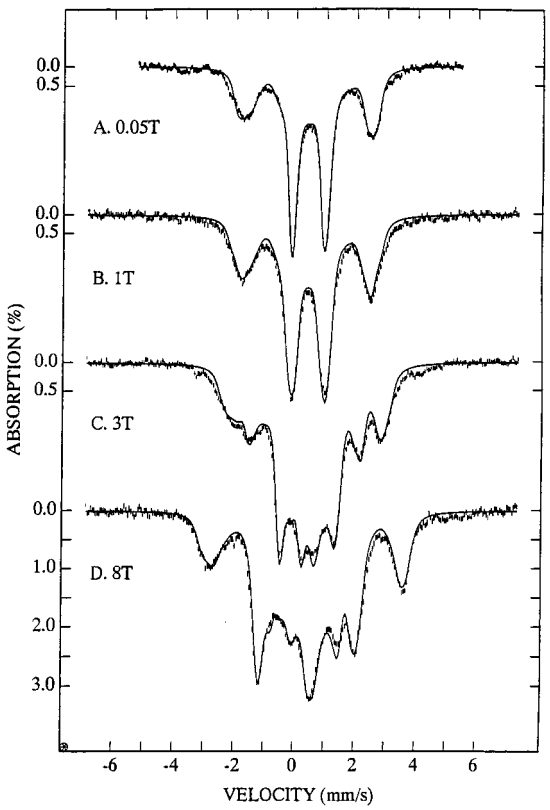

Figure 5. Mössbauer spectra of CO/CODH-treated α-subunit recorded at 4.2 K in the parallel applied fields indicated (same sample as in Figure 4).

The 4.2 K Mössbauer spectrum of Ni^{2+}-activated α-subunit from batch 3, shown in Figure 1B, exhibits a broad doublet that has the same isomer shift as that of Figure 1A, namely $\delta = 0.45$ mm/s. The broadening of the lines suggests that this doublet consists of a superposition of distinct but similar species. This preparation contained ∼60% nonlabile, 30% Ni-labile A-centers and, perhaps, 10% damaged A-centers (as determined by the method used to analyze a sample from batch 2, described in the next section). The broadening may be due to differences among these forms. Figure 1C shows an 8.0 T spectrum of the same sample. The simulation shown (solid line), generated by assuming that all iron sites are diamagnetic and have $\Delta E_Q = 1.08$ mm/s, matches the data well and shows that all clusters in the sample belong to an $S = 0$ system.

Mössbauer Studies of A_{red}-CO. A sample of Ni^{2+}-activated α-subunit from batch 2 was reduced with CO and a catalytic amount of CODH; the resulting Mössbauer and EPR spectra are shown in Figures 4−6 and 7A. The central doublet in the 90 K spectra of Figure 4B,C and in the 4.2 K spectrum of Figure 5A accounts for 47% of the total spectral intensity and almost certainly arises from $[Fe_4S_4]^{2+}$ clusters. Simulation of this component in the high-field spectra of Figure 5B−D shows that it is diamagnetic. One such simulation is presented in Figure 6B. Since Ni-labile A-clusters exhibit the pNiFeC signal in such samples and thus should contribute a Mössbauer spectrum exhibiting paramagnetic hyperfine structure, the diamagnetic component most probably arises from nonlabile A-clusters. Thus, CO/CODH appears unable to reduce this form of A-clusters.

The other major component of the Mössbauer spectra, corresponding to 40% of the spectral intensity, exhibits magnetic hyperfine splittings at 90 K. The pNiFeC signal of the A_{red}-CO state of the α-subunit belongs to an $S = {}^1/_2$ system with g-values at $g_x = 2.048$, $g_y = 2.046$, and $g_z = 2.021$ (see below). This signal, like its NiFeC counterpart of native CODH, does not broaden by relaxation at temperatures as high as 150 K. By contrast, all other species observed in the EPR spectra of the reduced α-subunit, including the $S = {}^3/_2$ and $S = {}^1/_2$ states evident in Figure 3A, have fast relaxing spins at such temperatures. Thus, at 90 K, the Mössbauer spectra of the A_{red}-CO state must exhibit magnetic hyperfine structure, while the other states exhibit quadrupole doublets. It follows that the magnetic components in the spectra of Figure 4B,C arise from the A_{red}-CO state.

The iron associated with A_{red}-CO is most readily identified in the 90 K spectra of Figure 4B,C, where it is responsible for the features around −2 and +2.5 mm/s Doppler velocity. The intensities of the Mössbauer spectra of species exhibiting isotropic EPR signals, such as the A_{red}-CO state, depend very sensitively on the direction of a weak (<0.1 T) applied magnetic field.[25] In contrast, species with integer electronic spin or fast relaxing Kramers systems such as the $S = {}^3/_2$ $[Fe_4S_4]^+$ cluster yield doublets whose intensity is not affected by the direction of the applied field. Thus, the difference spectrum obtained by subtracting the 90 K spectrum obtained in transverse field from that obtained in parallel field (Figure 4A) will contain only the contribution of A_{red}-CO, while those of all other species cancel.

The spectra also exhibit two minor components. One of these, corresponding to 3% of the iron in the sample, arises from a mononuclear high-spin Fe^{2+} contaminant ($\Delta E_Q \approx 3.1$ mm/s and $\delta \approx 1.35$ mm/s at 100 K). The high-energy line of

(25) Münck, E.; Huynh, B. H. In *ESR and NMR of Paramagnetic Species in Biological and Related Systems*; Bertini, I., Drago, R. S., Eds.; Reidel Publishing Co.: Dordrecht, Holland, 1979; pp 275−288.

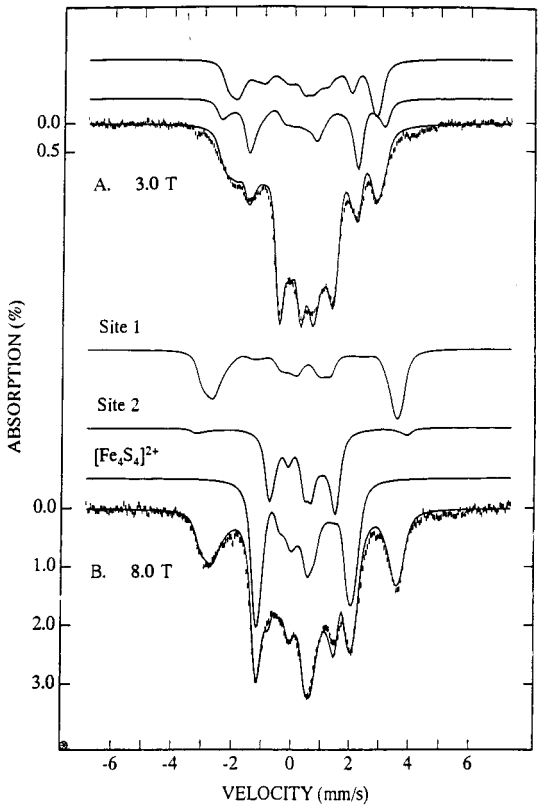

Figure 6. Decomposition of 4.2 K Mössbauer spectra of CO/CODH-treated α-subunit into subcomponents. Shown above the 3.0 T spectrum of A are the contributions of the two valence-delocalized pairs. The contribution of the diamagnetic $[Fe_4S_4]^{2+}$ fraction is indicated above the 8.0 T spectrum (B).

the doublet of the Fe^{2+} contaminant occurs at ∼+2.9 mm/s but is partly obscured by the more intense feature of A_{red}-CO. The low-energy line of the Fe^{2+} species, however, does not overlap with the low-energy feature of A_{red}-CO, and spectral simulations revealed readily that a small fraction of a high-spin contaminant must contribute at 2.9 mm/s velocity. The contribution of this contaminant has been removed from the spectra of Figures 4B,C and 5A.

If the spectra contained only contributions from the nonlabile A-center, A_{red}-CO, and the Fe^{2+} contaminant, the 90 K spectrum of Figure 4B would be identical to the 4.2 K spectrum of Figure 5A. We noticed, however, that the 4.2 K spectra contain an additional magnetic component with features similar to those of the spectrum of the dithionite-reduced α-subunit. Indeed, the low-temperature EPR spectra of the sample revealed the presence of some $S = {}^3/_2$ material. From analysis of the entire Mössbauer data set, we estimate that the $S = {}^3/_2$ species contributes ∼10% of the total absorption. For clarity, we have subtracted from the raw data a 10% contribution of the $S = {}^3/_2$ species, using the experimental spectra obtained for the reduced α-subunit.

We now turn to the analysis of the spectra associated with the $S = {}^1/_2$ system of A_{red}-CO. Figure 5 shows a series of spectra recorded in applied fields of different strength. The outer features of the A_{red}-CO spectrum broaden at 1.0 T and split at 3.0 T, revealing two distinct types of iron sites, one with positive components of the magnetic hyperfine tensor, **A**, and one with negative components. The overall features of the spectra suggest that the A-tensors of all iron sites are nearly isotropic. To determine ΔE_Q and δ for the iron sites of the A_{red}-CO, we have studied zero field spectra at 200 K, in hope that the electronic spin might relax fast enough at this temperature to permit

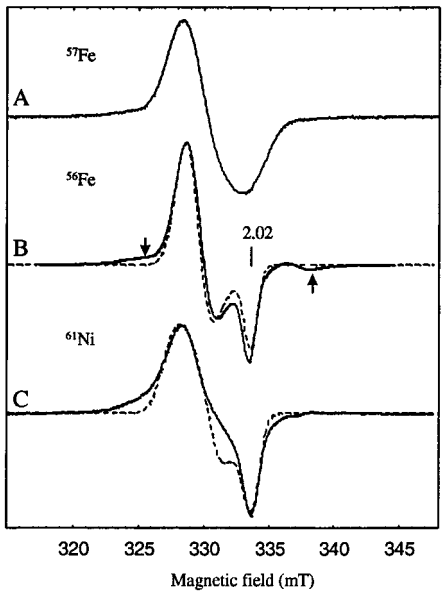

Figure 7. EPR spectra of α-subunit (the pNiFeC signal) after incubation with Ni and CO/CODH. (A) 80 K spectrum of ^{57}Fe-enriched α-subunit; the sample used is an aliquot of the Mössbauer sample of Figures 4−6. Conditions: microwave power, 40 μW; modulation amplitude, 2.2 mT. (B,C) pNiFeC signal of isolated α-subunit, prepared by discontinuous gel electrophoresis, after activation with Ni^{2+} in natural abundance (B) and ^{61}Ni (C); same spectra as shown in Figure 1B,C of ref 17. Dashed lines are spectral simulations using the following sets of *g*-values (Gaussian width): for B, 2.048 (1.65 mT), 2.046 (1.77 mT), and 2.021 (0.93 mT). For the spectrum in C, a ^{61}Ni magnetic hyperfine tensor was included; line width parameters were the same as in spectrum A. Parameters used for the *g*-values (*A*-tensor components): 2.048 (25 MHz), 2.046 (25 MHz), and 2.019 (10 MHz). Both EPR spectra contain an unidentified minority component with features around $g = 2.08$ and $g = 1.99$ (see arrows). This minority component was not present in the ^{57}Fe-enriched samples used in this study.

observation of quadrupole doublets. However, the spectrum was broad and featureless at 200 K, indicating an intermediate relaxation rate of the electronic system. Thus, ΔE_Q and δ had to be determined from analysis of the low-temperature spectra.

We have analyzed the spectra of A_{red}-CO with the $S = {}^1/_2$ spin Hamiltonian:

$$H = 2\beta \mathbf{S}\cdot\mathbf{H} + \sum_i \{\mathbf{S}\cdot\mathbf{A}_i\cdot\mathbf{I}_i - g_n\beta_n\mathbf{H}\cdot\mathbf{I}_i + (eQV_{zz}(i)/12)[3\mathbf{I}_{zi}^2 - 15/4 + \eta(i)(I_{xi}^2 - I_{yi}^2)]\} \quad (1)$$

where **S** is the spin operator of the cluster, $\mathbf{A}_i$ is the magnetic hyperfine tensor of site *i*, and $V_{zz}(i)$ and $\eta(i)$ are the *z*-component and asymmetry parameter, respectively, of the electric field gradient tensor of site *i*. In eq 1, $i = 1, 2$ sums over the two identified inequivalent spectral components (each representing a valence-delocalized pair of the Fe_4S_4 cluster, see below). The spectra of the diamagnetic $[Fe_4S_4]^{2+}$ cluster were analyzed with the same Hamiltonian by setting $\mathbf{A}_i = 0$. The solid lines in Figures 4−6 are the result of spectral simulations which yielded the parameters and fractions listed in Table 1. Overall, the parameter set describes the spectra very well. By adjusting the relative intensities of the various spectral components, we have determined the fraction of Fe belonging to A_{red}-CO. For the 90 K data, we found that 40 ± 2% of the ^{57}Fe in the sample belongs to A_{red}-CO. The 4.2 K data, however, uniformly required a slightly higher fraction, 43%, for the magnetic components. Presently, we do not understand this slight discrepancy. It is possible that some minority species, each,

Table 1. Parameters Used To Simulate the Mössbauer Spectra of CO-Reduced α-Subunit

cluster state	site	% of Fe	δ (mm/s)	ΔE_Q (mm/s)	η	A_x[a] (MHz)	A_y (MHz)	A_z (MHz)	A_{iso} (MHz)
A_{red}-CO	pair 1	20	0.46	1.32	0.8	+27.0	+29.2	+24.3	+26.8
	pair 2	20	0.46	1.10	1.1	−38.0	−36.0	−28.7	−34.2
A_{ox} (nonlabile)	site I	23.5	0.45	1.26	0.7				
	site II	23.5	0.45	0.96	0.65				

[a] Uncertainties for *A*-values are roughly ±2 MHz; because the *g*-values of A_{red}-CO are nearly isotropic, the *x,y,z* coordinates for pair 1 and pair 2 are not spatially correlated.

perhaps, accounting for only ∼1% of total Fe, may contribute magnetic features at 4.2 K and doublets at 90 K.

The isomer shifts of the two spectral components of A_{red}-CO are the same as those observed for the $[Fe_4S_4]^{2+}$ cluster of the *oxidized* α-subunit of Figure 1. Because the isomer shift is a very good marker for the oxidation state of the cluster, we have made efforts to determine this quantity from the fits as precisely as possible and found that δ cannot differ by more than ±0.02 mm/s from the values quoted in Table 1. The field dependence of the Mössbauer spectra can readily be modeled with a Hamiltonian that assumes an $S = {}^1/_2$ doublet well isolated in energy from the next higher state. Thus, the applied field does not appear to mix low-lying excited states into the ground doublet.

We have also analyzed spectra of activated α-subunit from batch 3. The spectral components observed had the same parameters, but the fraction of A_{red}-CO-associated Fe was only 28−30%, while the nonlabile A-center fraction accounted for ∼60%.

EPR Studies of A_{red}-CO. We have studied samples of CO-treated activated α-subunit with EPR between 4 and 170 K, both with and without ^{57}Fe enrichment. A representative EPR spectrum of the sample used for the Mössbauer study of Figures 4−6 is shown in Figure 7A. (The EPR and Mössbauer samples were prepared together in a glovebox and frozen within about 2 min of each other.) Because the sample was enriched in ^{57}Fe, the feature at $g = 2.05$ is not resolved from the resonance at $g = 2.02$. We have analyzed these spectra, together with wide-scan data, and have quantitated the double integral of the spectra against two independently prepared Cu^{II} EDTA standards. The intensity of the pNiFeC signal follows Curie behavior over the entire temperature range, suggesting that no other state is thermally accessible at temperatures up to 150 K. Quantitation of the pNiFeC signal yielded a spin concentration of 0.144 mM. Metal analysis by atomic absorption spectroscopy gave 2.25 mM Fe (average of two determinations, 2.40 and 2.10 mM). Given that the irons belong to an Fe_4S_4 cluster, and correcting for the 3% Fe^{2+} contaminant, this corresponds to 0.55 mM A-cluster and 0.26 spin/cluster. This spin concentration suggests that 26% of the cluster iron should belong to the Mössbauer spectrum associated with A_{red}-CO. However, as shown above, 40% of the cluster iron actually belongs to the magnetic components assigned to A_{red}-CO.

We have been unable to resolve this discrepancy. We have considered the possibility that it arose because EPR and Mössbauer samples were not prepared *identically*. To examine this, small fragments of material from the Mössbauer cup were pressed into an EPR tube, while maintaining the material under liquid nitrogen. After quantifying the EPR signal, the sample was thawed and analyzed for Fe. The resulting value of 0.27 spins/cluster agrees remarkably well with the previous result. Thus, the discrepancy between the EPR and Mössbauer results does not appear to arise from subtle differences in freezing the matched EPR and Mössbauer samples.

We also considered that this discrepancy might be unique to the particular sample examined. However, this is not the case. Our Mössbauer study with batch 3 of activated α showed that 28−30% of the cluster iron was associated with A_{red}-CO. The spin concentration obtained for this sample was also lower. Combining EPR quantitation, Mössbauer and metal analyses for this sample yielded 0.18 spin/cluster. Thus, a similar mismatch between the Mössbauer and EPR quantitation of A_{red}-CO was observed for both samples. Tbis discrepancy is not limited to the A-clusters of isolated α-subunits.[26]

We have also considered the possibility that some broader feature might be hidden under the pNiFeC signal. The EPR sample of batch 2 of ^{57}Fe-enriched α revealed a weak feature around $g = 2.3$ at temperatures between 80 and 150 K. The $g = 2.3$ resonance was absent in the sample from batch 3; its 130 K wide-scan EPR spectrum did not reveal any feature other than that attributed to the NiFeC signal.

Finally, we considered the possibility that the discrepancy between EPR and Mössbauer quantitation of A_{red}-CO was due to damaged A-clusters (or some contaminant) exhibiting magnetic hyperfine structure in the 90 K Mössbauer spectra. To examine this, the ^{57}Fe-enriched activated sample from batch 3 was thawed anaerobically, diluted, reconcentrated, reduced with CO/CODH, frozen, and reexamined by EPR and Mössbauer spectroscopy. For reasons not understood, samples treated in this manner do not attain the A_{red}-CO state. This sample was devoid of the pNiFeC signal and lacked magnetic features in the 90 K Mössbauer spectra. Thus, damaged A-clusters do not exhibit *magnetic* Mössbauer spectra at 90 K. Therefore, the discrepancy between the EPR and Mössbauer quantitation of the A_{red}-CO state does not appear to arise from a hypothetical A-cluster form that would exhibit magnetic spectral features at 90 K. In summary, we are presently unable to identify the reason why EPR spin quantitation of the NiFeC signal is consistently ∼30% less than the fraction of A_{red}-CO obtained by Mössbauer quantitation.

Parenthetically, at least 60% of the Fe in the diluted/reconcentrated sample belonged to diamagnetic $[Fe_4S_4]^{2+}$ clusters, and the remainder had features similar to those of $S = {}^3/_2$ $[Fe_4S_4]^+$ clusters. The diamagnetic fraction probably reflects nonlabile A-centers (which are not reducible by CO/CODH), and the remainder probably represents damaged and/or Ni-depleted A-clusters, suggesting that these A-cluster forms can be reduced to the $S = {}^3/_2$ state by CO/CODH.

The Mössbauer spectra show that the ^{57}Fe magnetic hyperfine interactions of the A_{red}-CO state are very similar to those observed for the A-cluster of the native CODH. In order to assess the ^{61}Ni magnetic hyperfine interactions, we have simulated the EPR spectra for two α-subunit samples that contained Ni in natural abundance (Figure 7B) and ^{61}Ni (>90%, Figure 7C). The simulation of the spectrum of Figure 7B yielded *g*-values at $g_x = 2.048$, $g_y = 2.046$, and $g_z = 2.021$.

(26) In our study of native CODH,[8] we found for a ^{57}Fe-enriched sample a spin concentration of 0.35 spin/αβ for the NiFeC signal, and 18% of the iron in the sample was associated with A_{red}-CO. Our current understanding suggests that each of the three CODH centers contains a Fe_4S_4 cluster. Thus, the Mössbauer results of CODH suggest a spin concentration of 18/33.3 = 0.56 spin/αβ, rather than the 0.38 spin/αβ observed. The magnitude of this discrepancy is similar to that observed here for activated α.

Except for the presence of a minority species with features at 2.08 and ~2.0 (apparently, this species was not present in our Mössbauer samples), the simulation matches the experimental features of the pNiFeC signal rather well. For the spectral simulation shown in Figure 7C, we have used the same line widths as for the natural abundance sample and, guided by the ENDOR results for native CODH of Fan *et al.*,[11] $A_x = A_y = 25$ MHz and $A_z = 10$ MHz for the ^{61}Ni hyperfine tensor. (The mismatch around $g = 2.04$ seems to reflect an underlying derivative feature belonging to the minority species.)

Discussion

In a seminal group of experiments, Ragsdale and co-workers demonstrated that the NiFeC signal of CODH broadened by hyperfine interactions when the enzyme was enriched in either ^{61}Ni or ^{57}Fe, or when it was treated with ^{13}CO.[9] They concluded that this signal originates from a Ni−Fe cluster, later called the A-cluster, that binds the substrate CO. Progress in delineating the structural features of the A-cluster has been slow, primarily because CODH preparations are heterogeneous in the sense that they contain different A-cluster populations. EPR studies[8a] revealed that the spin concentration of the NiFeC signal was consistently under 0.4 spin/$\alpha\beta$, while combined Mössbauer and EPR quantitations[8b] suggested that the Fe−S moiety of the A-cluster contained 5−6 Fe when the spin concentration was extrapolated to 1 spin/$\alpha\beta$. This was particularly puzzling since the values of ΔE_Q and δ were typical of those observed for $[Fe_4S_4]^{2+}$ clusters. Subsequently, Shin and Lindahl[6a] found that Ni of the A-cluster could be removed by phenanthroline and that removal of 0.3 Ni/$\alpha\beta$ abolished the NiFeC signal as well as the acetyl-CoA synthase activity of the enzyme. Since the amount of removable (labile) Ni correlated with the spin concentration of the NiFeC signal, it became apparent that the latter reflects a particular fraction of A-clusters (called Ni-labile) in a heterogeneous population of enzyme molecules.

Recently, Xia and Lindahl[27] developed a method of isolating the α-subunit and discovered that α exhibited an EPR feature with properties similar to those of the NiFeC signal.[17] This observation showed that the A-cluster of CODH was located in the α-subunit. With the modifications described above, we now achieve fairly high pNiFeC signal intensities, allowing us to study this cluster state in detail with Mössbauer spectroscopy.

The Mössbauer and EPR spectra of α reported here provide the most compelling evidence that the Fe−S species in α is an Fe_4S_4 cluster. In the oxidized state, the cluster is diamagnetic and exhibits a quadrupole doublet with an isomer shift of $\delta =$ 0.45 mm/s. This value is well within the range of δ values (0.43−0.47 mm/s) reported for $[Fe_4S_4]^{2+}$ clusters[28] (diamagnetic $[Fe_2S_2]^{2+}$ clusters have $\delta \approx 0.27$ mm/s,[28] and the nitrogenase P-clusters,[29] in the diamagnetic state P_N, have quadrupole patterns quite distinct from those of α). In the dithionite-reduced state, the Fe−S cluster of the nonlabile and damaged forms exhibits an $S = {}^3/_2$ ground state with Mössbauer and EPR properties typical of $[Fe_4S_4]^{+}$ clusters.[21,22] The values for ΔE_Q and δ obtained here match those of the $S = {}^3/_2$ $[Fe_4S_4]^{+}$ cluster of the Fe protein of nitrogenase. Although samples of oxidized α contain populations of different A-cluster forms, each form exhibits the same Mössbauer signature, namely that of an $[Fe_4S_4]^{2+}$ cluster. Moreover, the samples of Figure 1 do not contain any iron other than that assigned to the Fe_4S_4 cluster, ruling out the presence of a Ni−Fe−Fe_4S_4 assembly or a dinuclear Ni−Fe center, such as that observed in Ni−Fe hydrogenases.[30,31]

Our results regarding the nature of the Fe−S cluster are supported by the metal content of α along with its electronic spectra and X-ray absorption fine structure properties.[16] The amino acids ligating the A-cluster are still unknown, but there are six conserved cysteine residues in α that may serve this function.[32] Three or four cysteines are likely to coordinate the Fe_4S_4 cluster, while two or three cysteines may be ligands of the Ni site.[16]

Electronic Model for the $S = {}^1/_2$ A_{red}-CO State. The major aim of this study was to elucidate the electronic properties of the A_{red}-CO state of the A-cluster. A large body of data has established that the isomer shifts of Fe_4S_4 clusters are closely correlated to their oxidation states. Typical values for the average isomer shifts at 4.2 K are given below (variation ± 0.03 mm/s):

$$\underset{\delta = 0.31\ \text{mm/s}}{[Fe_4S_4]^{3+}} \overset{e^-}{\rightleftharpoons} \underset{\delta = 0.45\ \text{mm/s}}{[Fe_4S_4]^{2+}} \overset{e^-}{\rightleftharpoons} \underset{\delta = 0.57\ \text{mm/s}}{[Fe_4S_4]^{+}}$$

The shift observed for A_{red}-CO, $\delta = 0.46$ mm/s, is the same as that observed for the oxidized α-subunit, indicating that the $[Fe_4S_4]$ cluster is still in the 2+ state. Hence, the oxidation state of the cluster has not changed upon formation of A_{red}-CO, even though the cluster now exhibits paramagnetic hyperfine structure. In this section, we offer an explanation for these observations.

The Mössbauer data reveal that the iron sites occur in two distinct pairs. In the following, we focus on the isotropic parts of the magnetic hyperfine tensors, A_{iso}. The iron sites of one pair have negative *A*-values, $A_{iso} = -34.2$ MHz, while those of the other pair are positive, $A_{iso} = +26.8$ MHz. Note that the *A*-values of the pair with $A_{iso} < 0$ are larger in magnitude. For the (high-spin) tetrahedral iron sites of iron−sulfur clusters, positive *A*-values result when the local spin is aligned antiparallel to the cluster spin. Since the NiFeC signal is also broadened by ^{61}Ni, the data must be explained with a model that considers a Ni site with $S = {}^1/_2$ that is covalently linked to an $[Fe_4S_4]^{2+}$ cluster. The situation encountered here is similar to that described for the siroheme−$[Fe_4S_4]^{2+}$ assembly of *E. coli* sulfite reductase.[33,34] For the latter system, analysis of the Mössbauer data led to the conclusion that the siroheme iron is linked to the iron−sulfur cluster by a bridging ligand. This suggestion has been confirmed recently by crystallographic analysis of the enzyme, which revealed that the siroheme and the cluster are bridged by a cysteinyl sulfur.[35]

Although much work needs to be done, a variety of experimental and theoretical studies have clarified the electronic structure of $[Fe_4S_4]^{2+}$ clusters.[34,36,37] Thus, the ground state of the cluster comprises two valence-delocalized pairs, (A,B) and

(27) Xia, J.; Lindahl, P. A. *Biochemistry* **1995**, *34*, 6037−6042.
(28) Bertini, I.; Ciurli, S.; Luchinat, C. *Struct. Bonding*, **1996**, *83*, 1−56.
(29) Zimmermann, R.; Münck, E.; Brill, W. J.; Shah, V. K.; Henzl, M. T.; Rawlings, J.; Orme-Johnson, W. H. *Biochim. Biophys. Acta* **1978**, *537*, 185−207.
(30) Surerus, K. K.; Chen, M.; Van der Zwaan, W. J.; Rusnak, F. M.; Kolk, M.; Duin, E. C.; Albracht, S. P.; Münck, E. *Biochemistry* **1994**, *33*, 4980−4993.
(31) Volbeda, A.; Charon, M. H.; Piras, C.; Hatchikian, E. C.; Frey, M.; Fontecilla-Camps, J. C. *Nature* **1995**, *373*, 580−587.
(32) Maupin-Furlow, J. A.; Ferry, J. G. *J. Bacteriol.* **1996**, *178*, 6849−6856.
(33) (a) Christner, J. A.; Münck, E.; Janick, P. A.; Siegel, W. M. *J. Biol. Chem.* **1981**, *256*, 2098−2101. (b) Christner, J. A.; Münck, E.; Janick, P. A.; Siegel, L. M. *J. Biol. Chem.* **1983**, *258*, 11147−11156.
(34) Bominaar, E. L.; Hu, Z.; Münck, E.; Girerd, J.-J.; Borshch, S. *J. Am. Chem. Soc.* **1995**, *117*, 6976−6989.
(35) Crane, B. R.; Siegel, L. M.; Getzoff, E. D. *Science* **1995**, *270*, 59−67.
(36) Noodleman, L.; Peng, C. Y.; Case, D. A.; Mouesca, J.-M. *Coord. Chem. Rev.* **1995**, *144*, 199−244.
(37) Beinert, H.; Holm, R. H.; Münck, E. *Science*, **1997**, August 97.

(C,D), with spin $S_{AB} = S_{CD} = {}^9/_2$. The pair spin of ${}^9/_2$ is the result of distortion-enhanced double-exchange interactions (β_{intra}).[34] The two pair spins, in turn, are antiparallel coupled by Heisenberg−Dirac−VanVleck exchange (J_{cube}) to yield a diamagnetic ground state, designated as $|({}^9/_2,{}^9/_2);00\rangle$ using the $|(S_{AB}S_{CD});S_{cube}M\rangle$ nomenclature, where S_{cube} is the cluster spin. Theoretical studies of the sulfite reductase siroheme−$[Fe_4S_4]^{2+}$ assembly[34] show that the first excited cluster state is $|({}^9/_2,{}^9/_2);1M\rangle$. This excited state with $S_{cube} = 1$ is most relevant for the problem at hand.

Bominaar and co-workers[34] have developed an electronic model that explains the experimental data for the $S = {}^5/_2$ state of the coupled heme−cluster assembly of sulfite reductase. Belinsky, in a recent commentary[38] on double exchange, has reviewed this model and adopted a simplified version to describe the $S = {}^1/_2$ state of NO-complexed sulfite reductase. In the following, we consider a cubane in the 2+ state and assume that intrapair double exchange is so strong that the two iron sites of the pair remain equivalent when the Ni site is attached by a bridging ligand (Figure 8) to one of the irons of the $[Fe_4S_4]^{2+}$ cluster, Fe_D. We assume that the Ni site has spin $S_{Ni} = {}^1/_2$; whether this spin ${}^1/_2$ belongs to a localized Ni^+ site or whether spin density is substantially delocalized onto the ligands of the Ni need not be specified here. The exchange interaction between the Ni and Fe_D of the cluster (keeping the nomenclature of ref 34) can be described by an effective constant, j, $H_{NiFe} = j\mathbf{S}_{Ni}\cdot S_D$. The operator $\mathbf{S}_D$ mixes cluster states with $S_{cube} = 1$ into the cluster ground state. For strong intrapair double exchange, we can confine our considerations to the first excited state with $S_{cube} = 1$ at energy J_{cube}, where J_{cube} describes the antiferromagnetic interactions between the two delocalized pairs (J_{cube} is of order 200 cm^{-1}, see ref 34). Under the action of H_{NiFe}, the $S = {}^1/_2$ ground manifold of the system takes the following form:[38]

$$|\psi,M\rangle = \cos\alpha|S_{Ni}({}^9/_2,{}^9/_2)0;SM\rangle + \sin\alpha|S_{Ni}({}^9/_2,{}^9/_2)1;SM\rangle \quad (2)$$

where $\cos\alpha = [(\Gamma - x + 1)/2\Gamma]^{1/2}$, $\Gamma = [1 - 2x + 100x^2]^{1/2}$, and $x = j/4J_{cube}$.

The magnetic hyperfine coupling constants of the four iron sites, $i = 1, 4$, are obtained by computing $A_i = a_i\langle\psi,M|S_{iz}|\psi,M\rangle/M$ where the a_i are the intrinsic a-tensors (assumed to be isotropic) of the individual iron sites and the S_{iz} are the local spin operators. Using the results of Belinsky, the A_i-values can be written, after a correction:[39]

$$A_{A,B(C,D)} = \left\{\frac{1 - (1 - x)/\Gamma}{6} \pm \frac{33}{2}\frac{x}{\Gamma}\right\}a \quad (3)$$

where the + sign applies for sites A and B and the − sign for sites C and D. In Figure 9, we have plotted the magnitudes of $A_{A,B}/a$ (solid curve) and $A_{C,D}/a$ (dashed curve) as a function of j/J_{cube} for $j/J_{cube} > 0$. Equation 3 predicts that the A-values of the two delocalized pairs have opposite signs, in agreement with the experimental results. Moreover, the theory predicts that the pair with $A > 0$ has A-values of smaller magnitude, again in agreement with the experimental data. Because the same type of curves result for $j/J_{cube} < 0$, albeit with slightly smaller A-values for both pairs, one cannot deduce from the present data to which pair the Ni site is attached. For antiferromagnetic coupling, perhaps the more likely case here, the pair containing Fe_D would have $A_i > 0$. No matter whether j is positive or negative, the smaller A-values belong to the pair with $A > 0$. This is readily understood when one considers the limit for $j/J_{cube} \gg 1$.[40]

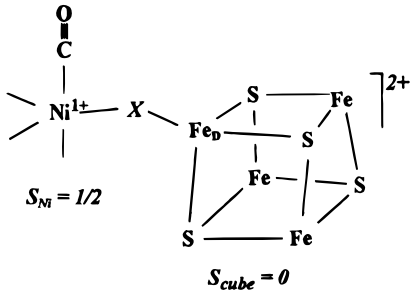

Figure 8. Schematic depiction of Ni−$[Fe_4S_4]^{2+}$ assembly of CODH A-center in the state that yields the NiFeC signal. No particular geometrical arrangement at the Ni^+ site is implied. For reasons discussed in the text, we favor the CO bound to the Ni^+.

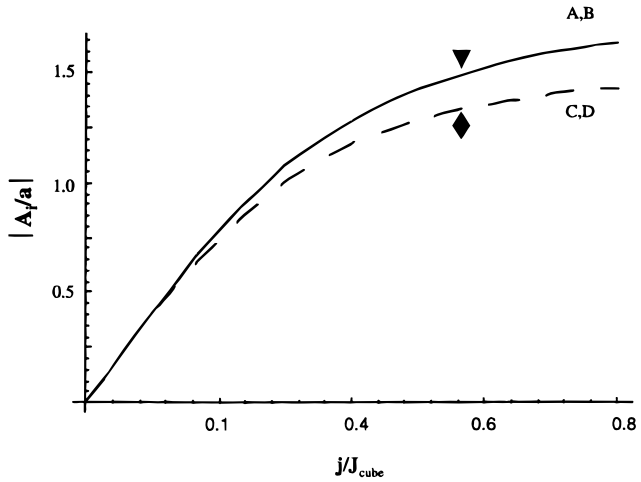

Figure 9. A-values of the two valence-delocalized pairs (A,B) and B,C) plotted as a function of j/J_{cube}. Plotted are $|A_{A,B}/a|$ and $|A_{C,D}/a|$ according to eq 3 for $j/J_{cube} > 0$, assuming that all iron sites have $a = -22$ MHz, $A_{A,B} < 0$, and $A_{C,D} > 0$. The Ni site is assumed to be linked to Fe_D. For $j/J_{cube} < 0$ (ferromagnetic coupling between the Ni and Fe_D), a similar plot results, with reversed signs for $A_{A,B}$ and $A_{C,D}$. Experimental data for the equivalent sites (C, D) of pair 1 (♦) and pair 2 (▼) are also plotted.

In order to determine the value for j/J_{cube}, we need the intrinsic hyperfine coupling constant, a. Analyses of the magnetic hyperfine interactions of the valence-delocalized pairs in $[Fe_3S_4]^0$ and $[Fe_4S_4]^{2+,3+}$ clusters suggest that $a = -22$ MHz (see Table 5 of Mouesca *et al.*[41]). By averaging the magnitudes of A_{iso} for both pairs, we obtain $|A_{av}| = 30.6$ MHz, which yields $j/J_{cube} = 0.56$ for $j > 0$ from eq 3. This result shows that the exchange coupling between the Ni site and the cube is substantial, namely $j \approx 110$ cm^{-1} if we adopt $J_{cube} = 200$ cm^{-1}. For $j/J_{cube} = 0.56$, we obtain from Figure 9 for $|A_{A,B}| - |A_{C,D}| = \Delta A = 3.5$ MHz,

(38) Belinsky, M. I. *J. Biol. Inorg. Chem.* **1996**, *1*, 186−188.

(39) Reference 38 contains a typographical error. In the expression for $\langle S_{1z,2z(3z,4z)}\rangle$, the quantity in brackets, $[1 - (1 - \gamma)/\Gamma]$, has to be divided by 12.

(40) For strong intrapair double exchange, the spin coupling reduces to a three-spin problem.[34] Consider a pair with $S_a = S_b = {}^9/_2$ that is coupled antiferromagnetically (J). Assume that the Ni site ($S_{Ni} = {}^1/_2$) is coupled (j) to site a. For $|j/J| \gg 1$, the ground state of the Ni−Fe_a pair has $S' = 4$ for $j > 0$ or $S' = 5$ for $j < 0$. Coupling of these states to S_b yields $S = {}^1/_2$ system states for which $A_a = -(44/15)a$, $A_b = +(55/15)a$ for $S' = 4$, and $A_a = +(54/15)a$, $A_b = -(45/15)a$ for $S' = 5$. For $a < 0$, the site with $A < 0$ has the largest magnitude of A in both cases. The branching of the curve in Figure 9 for values $j/J < 0$ "anticipates" the A-values for the limit $|j/J| \gg 1$.

(41) Mouesca, J.-M.; Noodleman, L.; Case, D. A.; Lamotte, B. *Inorg. Chem.* **1995**, *34*, 4347−4359.

which is somewhat smaller than the experimental value of 7.6 MHz. However, if we allow that the intrinsic *a*-values for the two pairs differ by, e.g., 10%, the experimental ΔA values are readily rationalized.

A comparison of the data obtained for the $S = {}^5/_2$ system of sulfite reductase[34] and the $S = {}^1/_2$ state considered here provides additional evidence for our model. The first term in eq 3 reflects the contribution of $\langle S_{Ni}({}^9/_2,{}^9/_2)1;SM|S_{iz}|S_{Ni}({}^9/_2,{}^9/_2)1;SM\rangle$ to the *A*-values. This matrix element has the same sign for all iron sites and is proportional to $\{S(S+1)\}^{-1}$. The second term in eq 3 results from the matrix elements $\langle S_{Ni}({}^9/_2,{}^9/_2)1,SM|S_{iz}|S_{Ni}({}^9/_2{}^9/_2)0,SM\rangle$, which are proportional to $\{S(S+1)\}^{-1/2}$. For the $S = {}^5/_2$ system of oxidized sulfite reductase, the contribution of the first term, which is responsible for branching of the curves in Figure 9, is suppressed, and, indeed, the experimental data show that $A_{12} \approx -A_{34}$.[33a,42] For the $S = {}^1/_2$ system of the NO complex of sulfite reductase, on the other hand, the *A*-values of the pairs have different values, $A_{iso}(1) = -25$ MHz and $A_{iso}(2) = +23$ MHz;[33b] these values correspond to $j/J_{cube} = 0.32$, with a predicted $\Delta A = 1.75$ MHz. Thus, the branching observed for the two $S = {}^1/_2$ systems reflects an intrinsic feature of the model.

The *g*-values of the coupled $S = {}^1/_2$ system are readily calculated from

$$g = \sum_{i=1,5} g_i \langle \psi,M|S_{iz}|\psi,M\rangle/M \text{ as } g = k_{Ni}g_{Ni} + k_{Fe}\sum_{i=1,4} g_{iFe} \quad (4)$$

where $k_{Ni} = [\Gamma - j/(2J_{cube}) + 2]/3\Gamma$ and $k_{Fe} = [\Gamma + j/(4J_{cube}) - 1]/6\Gamma$. The *g*-values of high-spin ferric FeS_4 sites are slightly above $g = 2.00$ ($\approx$2.02) and isotropic within $\pm$0.02, whereas those of ferrous FeS_4 sites range from 2.0 to 2.15.[43] Since the $[Fe_4S_4]^{2+}$ cube has (formally) two ferric and two ferrous sites, the average *g*-value for each pair will be close to $g_{av} \approx 2.05$. By replacing all g_{iFe} by g_{av} and using $j/J_{cube} = 0.56$, we obtain $g = 0.68g_{Ni} + 0.32g_{av}$. Writing $g_{Ni} = 2 + \Delta g_{Ni}$ and substituting in eq 4 yields

$$g \approx 2 + 0.68\Delta g_{Ni} \quad (5)$$

showing that the anisotropy of the intrinsic Ni *g*-tensor is scaled down ~30% by the coupling to the $[Fe_4S_4]^{2+}$ cluster. Thus, in view of the experimental *g*-values for the α-subunit, $g_x \approx g_y \approx 2.05$ and $g_z = 2.02$, we expect very small anisotropies of the intrinsic Ni *g*-tensor, the *g*-values being confined to the range 2.0−2.07 for the α-subunit and 2.03−2.11 for CODH. In an effort to model acetyl-CoA synthase activity, Holm and collaborators[44] have synthesized the trigonal-bipyramidal complex $[Ni(NS_3{}^{tBu})CO]^+$, where $NS_3{}^{tBu}$ = tris[(*tert*-butylthio)ethyl]-amine. This Ni^+ complex exhibits an axial $S = {}^1/_2$ EPR spectrum with $g_\perp = 2.119$ and $g_{||} = 2.008$, and is thus in the range required for A_{red}-CO. Finally, our model yields for the ^{61}Ni magnetic hyperfine tensor of the coupled system $\mathbf{A}_{Ni} = k_{Ni}\mathbf{a}_{Ni} \approx 0.68\mathbf{a}_{Ni}$, suggesting that $a_x \approx a_y \approx 37$ MHz and $a_z \approx 15$ MHz.

Presence of Distinct A-Cluster Forms and Spin Quantitation of the pNiFeC Signal. Both Ni-labile and nonlabile forms of the A-cluster are EPR-silent in the oxidized state and contain the Fe_4S_4 cluster in the 2+ state. The lack of an EPR signal indicates that the nickel is in the divalent state. The Fe_4S_4 moiety of nonlabile A-clusters can be reduced by dithionite to the $S = {}^3/_2$ $[Fe_4S_4]^+$ state; these A-clusters, however, are not reduced by CO/CODH. Thus, the fraction of α-subunits with nonlabile A-clusters (~47% for the batch 2 sample of Figures 4−6 and 60% for the sample of batch 3) does not contribute to the pNiFeC signal; this signal arises exclusively from the Ni-labile form of the A-cluster.

The substoichiometric spin concentrations obtained for the NiFeC signal of CODH have puzzled researchers for more than 10 years. The present study has shown that the major reason for this low spin concentration is that only ~30%−40% of α-subunits, namely those with undamaged Ni-labile A-clusters, can exhibit the signal. This discovery largely solves the puzzle of the low spin concentration for the A-cluster of CODH. However, even after this factor is taken into account, the spin concentrations remain lower than expected from analysis of the Mössbauer spectra (27% lower for batch 2 and 35% lower for batch 3). We have considered a variety of possibilities to explain this, including saturation effects, broad features underlying the main EPR signal, errors in the double integration of the EPR signal caused by baseline problems, inaccurately prepared Cu standards, and the presence of low-lying electronic states that may have led to a depopulation of the doublet that yields the pNiFeC signal. We have also considered that the Fe−S moiety in the A-cluster may actually be a novel structure with 5−6 irons (that happens to display Mössbauer and EPR properties identical to those of $[Fe_4S_4]^{2+/+}$ clusters) and that the pNiFeC signal develops only when two α-subunits interact. However, none of these explanations appears compatible with the data, and this minor discrepancy thus remains unexplained. There are other examples where substoichiometric spin concentrations have been obtained. For instance, the $[Fe_3S_4]^+$ cluster of inactive aconitase, whose Mössbauer spectra we understand very well, yields an EPR signal that persistently has a spin concentration of ~0.7 spin/$[Fe_3S_4]^+$ (H. Beinert, personal communication).

The nonlabile and Ni-labile forms of the A-cluster were present in both ^{57}Fe-enriched preparations examined by Mössbauer spectroscopy (batches 2 and 3), and the low spin concentrations obtained for every sample of isolated α studied to date suggest that all samples contain heterogeneous populations of A-clusters. Using EPR spin concentration and 0.7 spin/[Ni-labile A-cluster] as an empirical conversion factor, we estimate that, for most of our samples, ~40% of A-clusters are Ni-labile and 60% are nonlabile. Depending on the history of the sample (how it was prepared, whether it had been diluted or exposed to oxygen or phenanthroline), a portion of the Ni-labile form may be damaged or Ni-depleted and unable to exhibit the pNiFeC signal.

Viewed from this perspective, the ^{57}Fe-enriched sample prepared by discontinuous gel electrophoresis (batch 1, the sample of Figures 1A and 3) probably contained ~60% nonlabile and ~40% damaged A-centers. Since >95% of the Fe_4S_4 clusters of the sample of Figure 1 were reduced into the $S = {}^3/_2$ state, damaged A clusters would appear to have redox properties similar to those of the nonlabile form. However, further studies are underway to examine this. Based on our current understanding, the samples used for the X-ray absorption study of Xia *et al.*[16] are likely to have contained a mixture of nonlabile and damaged A-clusters. Consequently, their result indicating that "*the*" Ni site in α has a distorted square-planar geometry with two S and two N/O ligands now must be viewed as referring to some "*average*" geometry of the Ni sites in nonlabile and damaged A-clusters. Most importantly, this analysis indicates that the geometry of the Ni site in the Ni-labile form remains undetermined.

(42) Cline, J. F.; Janick, P. A.; Siegel, L. M.; Hoffman, B. M. *Biochemistry* **1985**, *24*, 7942−7947.
(43) Bertrand, P.; Gayda, J.-P. *Biochim. Biophys. Acta* **1979**, *579*, 107−121.
(44) Stavropoulos, P.; Muetterties, M. C.; Carrie, M.; Holm, R. H. *J. Am. Chem. Soc.* **1991**, *113*, 8485−8492.

Comments on Coupling in the Oxidized States of the A-Cluster. We have not been able to determine whether the Ni and the Fe_4S_4 cube are linked by a bridge in the *oxidized* states. Oxidized α is EPR silent, and the Fe_4S_4 cluster is in the diamagnetic 2+ state. The absence of an EPR signal indicates that the nickel sites (from nonlabile, Ni-labile, and damaged forms) are Ni^{2+}. If the Ni^{2+} were low-spin ($S_{Ni} = 0$), the A-center would be diamagnetic, and the Mössbauer spectra would not reveal whether the Ni site is covalently linked to the cluster. For high-spin ($S_{Ni} = 1$) Ni^{2+}, on the other hand, exchange-coupling between the Ni^{2+} and the cluster could yield ^{57}Fe magnetic hyperfine interactions if the spectra were studied in strong applied magnetic fields. The expected hyperfine fields at the iron sites would be proportional to $(\beta H/D)(j/J_{cube})$, where D is the zero field splitting parameter of the Ni^{2+}. The situation described occurs for the Fe^{2+} siroheme−$[Fe_4S_4]^{2+}$ assembly of $1e^-$ reduced sulfite reductase; for the latter system, an $S = 1$ siroheme iron is linked to an $[Fe_4S_4]^{2+}$ cluster, and coupling was readily observed with Mössbauer spectroscopy.[33b] As shown in the Results, the 8.0 T spectrum of the Ni-activated α-subunit is fit well with the assumption that all iron in the sample resides in a diamagnetic environment. Thus, we have no direct evidence that the Ni site is covalently linked to the Fe_4S_4 cluster in the nonlabile and Ni-labile forms. If they are linked, the Ni must be low-spin $S_{Ni} = 0$; if they are not linked, the Ni may be either low- or high-spin.

Comparison of the A-Cluster in Isolated α with That in Native $\alpha_2\beta_2$ Enzyme. The results obtained here for the A-cluster of the isolated α-subunit are nearly identical to those reported for the A-cluster of the native enzyme. Our previous studies of the enzyme, at lower resolution due to heterogeneities in both the A- and C-centers and the presence of the B-cluster, have elicited Mössbauer parameters for the A_{red}-CO state, $A_{iso}(1) = -32.2$ MHz and $A_{iso}(2) = 27.8$ MHz,[8b] similar to those reported here. We have proposed previously that the A-cluster may have a structure as depicted in Figure 8, but the difficulties of obtaining quantitative data for CODH, together with a lack of understanding of the electronic structure of $[Fe_4S_4]^{2+}$ cubanes, prevented us from developing a detailed electronic model. Q-band ENDOR studies by Fan and co-workers[11] indicate that the A-center contains either one type of iron with $A_\perp = 35$ MHz and $A_{||} = 27$ MHz, or two types of Fe with $A(1) = 35$ MHz and $A(2) = 27$ MHz. The Mössbauer data show that the latter assignment is the correct choice. Using ENDOR *A*-values, Fan *et al*. performed EPR simulations of the NiFeC signal and concluded that the A-center contains 3−4 Fe sites. Our values obtained for the ^{61}Ni hyperfine tensor of the pNiFeC signal are, within the uncertainties, identical to the ENDOR data reported by Fan *et al*. for the A-center of native enzyme. Given the similarities of the enzyme and α-subunit data, we conclude that the A_{red}-CO state of isolated α is essentially the same as that of native enzyme.

The different forms of the A-cluster observed in isolated α are also present in native enzyme. The Ni-labile A-cluster in native enzyme yields an EPR very similar to that of isolated α, with similar substoichiometric spin intensity.[25] The ratio of Ni-labile and nonlabile A-clusters in the native enzyme also appears to be similar to that in isolated α. (The nonlabile A-clusters of the native enzyme are indicated by the bracket in Figure 5 of Lindahl *et al*.[8b]) Moreover, dithionite-reduced native enzyme exhibits $S = {}^3/_2$ EPR features, as would be expected if some of its A-clusters were of the nonlabile type. However, this evidence must be tempered by the possibility that some or all of those features may originate from C and B clusters.

CO Binding to Ni-Labile A-Clusters. The ^{13}C hyperfine broadening of the NiFeC EPR signal established that CO or some derivative thereof was bound to the A-cluster (in the A_{red}-CO state). Ragsdale and Wood[9c] proposed that the CO and the methyl used in synthesizing acetyl-CoA bind to the Ni of the A-cluster and that the two substrates react via a migratory insertion to generate a Ni-acetyl intermediate, which is subsequently attacked by CoA to yield acetyl-CoA. This proposal is supported by studies of the migratory insertion mechanisms of well-characterized systems, in that they occur with substrates bound at adjacent positions at the same metal center. This mechanism has also been supported by studies which indicate that the methyl group binds to the Ni of the Ni-labile A cluster.[45,46] Thus, it came with some surprise that Qiu *et al*.[47] recently concluded, from a resonance Raman study of CODH, that CO binds to an Fe of the A-cluster rather than to the Ni. The authors observed a band at 360 cm^{-1} that shifted when ^{13}CO or C^{18}O was used, or when the Fe−S clusters were enriched in ^{54}Fe (^{54}Fe shifted the resonance by 2 cm^{-1}; ^{61}Ni substitution did not produce an observable shift). They subsequently found that this 360 cm^{-1} feature, assigned to an Fe−CO stretch, developed at the same rate as the NiFeC signal when CODH was exposed to CO.[48] $[Fe_4S_4]^{2+}$ clusters generally exhibit characteristic resonance Raman bands.[49] These bands are also observed for the *coupled* siroheme−$[Fe_4S_4]^{2+}$ chromophore of sulfite reductase.[50] Since no Fe−S cluster modes were observed in the state yielding the 360 cm^{-1} feature, Qiu *et al*. concluded that the Fe_4S_4 cluster of A_{red}-CO was in the reduced 1+ state. This apparently selective resonance enhancement of an $[Fe_4S_4]^+$-CO band was also surprising, since resonance Raman bands have not been observed for any $[Fe_4S_4]^+$ cluster,[51] and because CO is not known to bind to such clusters. These authors displayed a model in which CO was bound to one Fe of the cube, resulting in a five-coordinate Fe site.

We have considered whether CO binding to an iron site of the A-center would produce a distinctive Mössbauer signature. Holm and collaborators[52] have studied a variety of $[Fe_4S_4]^{2+}$ cubanes containing a five-coordinate Fe site and found that formation of such sites leads to isomer shifts ranging from 0.62 to 0.96 mm/s, compared to $\delta = 0.45$ mm/s for a tetrahedral iron site. We would have readily recognized such a site in the spectra of A_{red}-CO if CO were bound to the bridging Fe_D as considered by Qiu *et al*.[48] On the other hand, one could consider a situation where CO would replace an endogenous ligand such as the cysteinate sulfur with retention of tetrahedral symmetry around the Fe site. Although we would expect observable changes in ΔE_Q and δ for this particular site, we cannot rule out this possibility, because suitable model complexes are not available. Our Mössbauer studies unambiguously show that the state which exhibits the NiFeC signal, namely A_{red}-CO, contains an Fe_4S_4 cluster in the 2+ core oxidation state. If the A-cluster state that yields the 360 cm^{-1} resonance Raman band contains

(45) Kumar, M.; Qiu, D.; Spiro, T. G.; Ragsdale, S. W. *Science* **1995**, *270*, 628−630.
(46) Barondeau, D.; Lindahl, P. A. *J. Am. Chem. Soc*. **1997**, *119*, 3959−3970.
(47) Qiu, D.; Kumar, M.; Ragsdale, S. W.; Spiro, T. G. *Science* **1994**, *264*, 817−819.
(48) Qiu, D.; Kumar, M.; Ragsdale, S. W.; Spiro, T. G. *J. Am. Chem. Soc*. **1995**, *117*, 2653−2654.
(49) Czernuszewicz, R. S.; Macor, K. A.; Johnson, M. K.; Gewirth, A.; Spiro, T. G. *J. Am. Chem. Soc*. **1987**, *109*, 7178−7187.
(50) Madden, J. F.; Han, S.; Siegel, L. M.; Spiro, T. G. *Biochemistry* **1989**, *28*, 5471−5477.
(51) Spiro, T. G.; Czernuszewicz, R. S.; Han, S. In *Biological Applications of Raman Spectroscopy*; Spiro, T. G., Ed.; Wiley-Interscience: New York, 1988; Vol. 3, pp 523−554.
(52) Holm, R. H.; Ciurli, S.; Weigel, J. A. *Prog. Inorg. Chem*. **1990**, *38*, 2−64.

an $[Fe_4S_4]^{1+}$ cluster, as suggested by Qiu *et al*., then that state, according to our results, would not appear to be A_{red}-CO.

Because CO is not known to bind to *reduced* $[Fe_4S_4]^{+}$ clusters, and given the lack of Mössbauer evidence for an $[Fe_4S_4]^{2+}-$CO adduct in isolated α, we consider it unlikely that CO is bound to Fe in A_{red}-CO. Given also that Ni^{+}-CO adducts are well documented in the literature, we prefer to coordinate the CO to the Ni^{+} site (Figure 8). (We understand that this does not solve the problem of the 360 cm^{-1} resonance Raman line, but this line may report a cluster state different from A_{red}-CO.) Finally, given the very similar properties of the A-cluster in isolated α and native enzyme, it seems very unlikely that CO is bound to Fe in native enzyme and to Ni in isolated α.

Differences between Ni-Labile and Nonlabile A-Clusters. The results of Shin *et al*.[7] and the present results show that native CODH as well as the isolated α-subunit preparations contain Ni-labile and nonlabile A-clusters. The different reactivities of these forms toward phenanthroline and CO point to structural differences which remain to be elucidated. It is clear that this issue has profound implications for understanding the catalytic mechanism of the enzyme. As shown by Shin *et al*.,[12] different A-cluster populations do not arise during purification of the enzyme; they are already present in crude cell extracts. Mössbauer and EPR spectroscopy, taken together, are excellent tools for keeping track of the different A-cluster forms. We are pursuing further studies to elucidate the structural differences and possible conversion between the two forms.

Summary

The principal conclusions of this study are as follows: (a) isolated α-subunits contain an Fe_4S_4 cluster and a Ni center, and these constitute the A-cluster; (b) in the oxidized state (A_{ox}), the Ni is in the Ni^{2+} state and the cube is in the diamagnetic $[Fe_4S_4]^{2+}$ state; (c) preparations of α-subunits contain two major forms of the A-cluster, called Ni-labile and nonlabile; (d) Ni-labile A-clusters are catalytically active[17] (when associated with β-subunits in native enzyme), contain a Ni that can be removed by phenanthroline, and can be reduced by CO/CODH to the $S = {}^1/_2$ A_{red}-CO state, which exhibits the pNiFeC signal; (e) nonlabile A-clusters are catalytically inactive, contain a Ni that is not removed by phen, and cannot be reduced by CO/CODH, but can be reduced by dithionite to an $S = {}^3/_2$ state in which the cube is an $[Fe_4S_4]^{+}$; (f) in the $S = {}^1/_2$ A_{red}-CO state, the cube is in the oxidized $[Fe_4S_4]^{2+}$ state and the Ni is in the reduced Ni^{+} state; (g) the low spin concentration obtained for the NiFeC signal arises largely because of the proportion of A-clusters in the nonlabile form, which does not contribute to the signal; (h) the same two forms of the A-cluster are present in native CODH; (i) if CO is bound to the cube of the A-cluster in the A_{red}-CO state, as has been proposed by Qiu *et al*.,[47] it must replace a ligand to the cluster retaining a four-coordinate Fe site; and (j) the structural difference responsible for the different catalytic and spectroscopic properties of the Ni-labile and nonlabile A-cluster is unknown but may involve different ligand environments at the Ni sites.

Acknowledgment. This work was supported by grants from the National Institutes of Health, GM 22701 (to E.M.) and GM 46441 (to P.A.L.), and the National Science Foundation, MCB-9406224 (to E.M.).

Note Added in Proof. The theory presented above may shed some light on the structure of the H-cluster of Fe-hydrogenases. The H-cluster contains approximately six Fe atoms (Adams, M. W. W. *Biochim. Biophys. Acta* **1990**, *1020*, 115−145). Mössbauer studies of the $S = 1/2$ state of the H-cluster of CO-complexed hydrogenase II from *C. pasteurianum* have revealed the presence of two pairs of Fe sites; one pair has $A = -30$ MHz and the other $A = +26.5$ MHz (Rusnak, F. M.; Adams, M. W. W.; Mortenson, L. E.; Münck, E. *J. Biol. Chem.* **1987**, *262*, 38−41). The isomer shifts of both pairs are the same as those of $[Fe_4S_4]^{2+}$ clusters. The above *A*-values, for $j/J_{cube} \approx 0.44$, fit the theoretical curves of Figure 9, suggesting that it may be fruitful to pursue the idea that the H-cluster is an assembly consisting of a moiety comprised of one to two Fe atoms (that carry the $S = 1/2$ spin) exchange-coupled to an Fe_4S_4 cluster. It is tempting to speculate that this putative Fe_4S_4 cluster is evolutionary related to the proximal Fe_4S_4 cluster (31) of Ni−Fe-hydrogenases.

JA971025+